

## Stimulated cooperative Jahn-Teller effect in $\text{TmPO}_4$

P. Morin

*Laboratoire Louis-Néel, CNRS, 166X, 38042, Grenoble Cedex, France*

Z. Kazei

*Laboratory for Magnetism, Physics Department, Moscow State University, 119899, Moscow, Russia*

(Received 7 October 1996)

The idea of stimulating a cooperative Jahn-Teller effect in undercritical electronic systems using an external stress, which does not belong to the symmetry of the quadrupolar ordering, was recently suggested theoretically. The rare-earth oxide compound  $\text{TmPO}_4$  (tetragonal zircon structure) is discussed here. The role of the external stress, a magnetic field applied along the  $[100]$  axis, is to bring the  $\delta$ -symmetry quadrupolar component to criticality by the reconstruction of both the levels spacings and the eigenfunctions. The thermodynamical properties are obtained by considering all the characteristics of the magnetoelastic couplings and of the crystalline electric field. The structural phase diagram exhibits reentrant transitions between the tetragonal and orthorhombic symmetries. The measurements of the magnetic vector and of the magnetostriction induced by the magnetic field are well described within this model. The simultaneous measurement of the components of the magnetic moment parallel and perpendicular to the field is an interesting experimental technique, efficient for the investigation of quadrupolar interactions. [S0163-1829(97)05114-X]

### I. INTRODUCTION

The studies of magnetoelastic properties soared in popularity in the 1970's for insulating compounds. Rare-earth ( $R$ ) orthophosphates and orthovanadates with the zircon structure are now considered as archetypes of the cooperative Jahn-Teller (JT) effect. Several of them,  $\text{DyVO}_4$ ,  $\text{TbVO}_4$ ,  $\text{TmVO}_4$ , and  $\text{TbPO}_4$  for instance, exhibit a spontaneous tetragonal-orthorhombic transition.<sup>1</sup> Large magnetoelastic couplings are also present in  $R$  intermetallics and compete with the other magnetic interactions; structural transitions are observed in the paramagnetic range of  $\text{TmZn}$  and  $\text{TmAg}_2$ . This coexistence has made necessary the development of microscopic models considering both types of interactions, quadrupolar and magnetic, in the presence of the crystalline electric field (CEF).<sup>2,3</sup> The subject of JT effects has recently known a new impulse of interest in relation to structural phase transitions in high-temperature superconductors, fullerenes, and manganites.<sup>4-6</sup> Progress in the understanding of the electron-electron correlations mediated by phonons is thus of great interest and rare-earth compounds constitute a favorable field for further developments. Indeed the CEF determines very different conditions for the existence of the quadrupolar ordering according to the level and eigenfunction configurations.

However the absence of a spontaneous JT transition in spite of sizable magnetoelastic interactions also constitutes an interesting situation. This concerns undercritical systems where the energy gap between the nonquadrupolar ground-state and excited levels quadrupolarly active is larger than the magnetoelastic interactions. In such a case, the structural phase transition can be stimulated by an external stress driving the electronic system to the critical state.<sup>7,8</sup> Since the JT interactions cannot be significantly increased, the equality can be achieved by reducing the energy gap. The original feature of the model developed in Refs. 7 and 8 for the

stimulated JT transition comes from the fact that the reconstruction of the level spectrum is driven by an external stress, which does not belong to the same symmetry as the quadrupolar component liable to order: as long as the critical state is not reached, the quadrupolar moment remains zero.  $\text{TmPO}_4$  was predicted to be a favorable candidate for the first evidence of such a stimulated transition. Indeed, it belongs to the family of so-called four-level systems. The low-lying electronic states are two singlets at 0 and 110 K and a non-Kramers doublet at 41.6 K.<sup>9</sup> The magnetoelastic contribution for the  $C_{66}$  elastic mode induces a softening of about 85% around 20 K. This strong, but nonzero dip indicates that  $\text{TmPO}_4$  does not undergo a spontaneous quadrupolar ordering, but remains undercritical.<sup>10</sup>

Note that the stimulated cooperative JT effect must not be confused with the case of a same-symmetry stress: as soon as applied in the disordered phase, this latter induces a nonzero value for the corresponding quadrupolar component, which is reinforced by the quadrupolar interactions. This avalanche effect is observed for instance for the quadrupolar components of the  $\gamma$  ( $B_{1g}$ ) symmetry in a magnetic field applied along a  $[100]$  axis in cubic  $\text{TmZn}$  or in tetragonal  $\text{TmAg}_2$ .<sup>3</sup>

We have recently determined the different magnetoelastic couplings considering all the features of the CEF of the ground-state multiplet in  $\text{TbPO}_4$  (Ref. 11) and in  $\text{TmPO}_4$ .<sup>12</sup> This approach, based on a susceptibility formalism, allows us a general understanding of the magnetic and magnetoelastic properties in an entire family of compounds contrary to the case of pseudospin models, which have to be adapted to the compound under consideration. In both compounds, the magnetoelastic coefficients associated with each of the different symmetry lowering modes are comparable in magnitude and the  $\delta$  ( $B_{2g}$ ) orthorhombic mode dominates the other ones. The occurrence of the  $\delta$ -symmetry quadrupolar ordering in  $\text{TbPO}_4$  and its absence in  $\text{TmPO}_4$  are discussed in Ref.

12. We present here, how the  $\delta$  quadrupolar ordering, i.e., the orthorhombic deformation of the tetragonal cell along its [110] direction, is stimulated by a magnetic field applied along the [100] tetragonal axis. In the next section, we briefly recall the formalism describing the properties of the  $4f$  shell and discuss the mechanism of the stimulated JT transition in  $\text{TmPO}_4$ . We then present the signature of this effect seen in the magnetic and magnetostrictive properties (Secs. III and IV, respectively).

## II. STRUCTURAL PHASE DIAGRAM

The magnetic properties of the  $4f$  shell are described with the usual Hamiltonian using the equivalent operator method<sup>13</sup> and the mean-field approximation (MFA):

$$\mathcal{H} = \mathcal{H}_{\text{CEF}} + \mathcal{H}_M + \mathcal{H}_{\text{ME}} + \mathcal{H}_Q + E_{\text{el}} + E_Q. \quad (1)$$

It includes the CEF term, one and two ion couplings for both the magnetic and quadrupolar couplings.<sup>2</sup> The CEF term is written within a system of  $x, y, z$  axes parallel to the [100], [010], and [001] directions of the lattice cell, respectively. The CEF parameters are the same as used in Ref. 12. The magnetic term,  $\mathcal{H}_M$ , reduces here to the Zeeman coupling to the applied magnetic field,  $\mathbf{H}$ , the bilinear interactions being negligible in  $\text{TmPO}_4$ . Only magnetoelastic contributions linear in strain and restricted to second-rank terms are considered here. They can be written in symmetrized notations as<sup>14</sup>

$$\begin{aligned} \mathcal{H}_{\text{ME}} = & -(B^{\alpha 1} \epsilon^{\alpha 1} + B^{\alpha 2} \epsilon^{\alpha 2}) O_2^0 - B^\gamma \epsilon^\gamma O_2^2 - B^\delta \epsilon^\delta P_{xy} \\ & - B^\epsilon (\epsilon_1^\epsilon P_{zx} + \epsilon_2^\epsilon P_{yz}), \end{aligned} \quad (2)$$

$\alpha, \gamma, \delta$ , and  $\epsilon$  correspond to the tetragonal, orthorhombic, and monoclinic symmetry modes.  $O_2^0, O_2^2, P_{ij}$  are the quadrupolar Stevens operators, the  $B^\mu$ 's are the magnetoelastic coefficients, which are temperature independent.  $E_{\text{el}}$  is the related elastic energy.<sup>2</sup> The two-ion quadrupolar terms are written as

$$\begin{aligned} \mathcal{H}_Q = & -K^\alpha \langle O_2^0 \rangle O_2^0 - K^\gamma \langle O_2^2 \rangle O_2^2 - K^\delta \langle P_{xy} \rangle P_{xy} \\ & - K^\epsilon [\langle P_{yz} \rangle P_{yz} + \langle P_{zx} \rangle P_{zx}]. \end{aligned} \quad (3)$$

Minimizing the free energy with regard to the strains gives the equilibrium strains as functions of the expectation values of the corresponding quadrupolar operators. Replacing the equilibrium values for the  $\epsilon^\mu$ 's makes Eq. (2) indistinguishable from Eq. (3) and leads to the total quadrupolar coefficients:

$$G^\mu = \frac{(B^\mu)^2}{C_0^\mu} + K^\mu \quad (\mu = \gamma, \delta, \epsilon) \quad (4)$$

$C_0^\mu$  being the background elastic constants. The corrective energy  $E_Q$  arises from the fact that each rare-earth pair is counted twice in the MFA treatment of the quadrupolar pair interactions:  $E_Q = 1/2 K^\delta \langle P_{xy} \rangle^2$  for the  $\delta$  symmetry.

In the presence of small external stresses, perturbation theory can be applied to the disordered phase. The free energy is then analytically expressed using three single-ion susceptibilities associated with each of the symmetry lowering modes. They depend only on the CEF. For instance for the  $\delta$  symmetry, the strain susceptibility can be written as

$$\chi_\delta = \sum_{i,k} f_i \left[ -2 \sum_{j \neq i,l} \frac{|P_{ik,jl}|^2}{E_i - E_j} + \frac{1}{k_B T} |P_{ik,ik}|^2 \right]. \quad (5)$$

$P_{ik,jl}$  are the matrix elements of the  $P_{xy}$  operator,  $E_i$  and  $f_i$  are the energy and the Boltzman factor of the  $i$  level. It is responsible for the softening of the  $C^\delta = 2C_{66}$  elastic constant,  $C^\delta/C_0^\delta = (1 - G^\delta \chi_\delta)/(1 - K^\delta \chi_\delta)$ . The various  $B$ 's,  $K$ 's, and  $G$ 's can be also determined from the parastriction and third-order magnetic susceptibility.<sup>2</sup> As soon as the magnetoelastic coefficients are known, it is then possible to describe the properties observed under large external stresses by self-consistent diagonalization of Eq. (1).

All the magnetoelastic coefficients are known in  $\text{TmPO}_4$ .<sup>12</sup> For instance, for the orthorhombic symmetry lowering modes,  $B^\gamma = 78$  K ( $G^\gamma = 6$  mK) and  $B^\delta = -151$  K ( $G^\delta = 130$  mK). The values of  $G^\delta$  and  $G^\gamma$  are very different due to the differences between the magnetoelastic constants, but also between the  $C_\delta^0$  and  $C_\gamma^0$  background elastic constants. Since in  $\text{TmPO}_4$ , the values of the  $\langle O_2^2 \rangle$  quadrupolar operator and related susceptibilities are small, the contribution to the free energy of the  $\gamma$  symmetry lowering mode is weak in comparison to the  $\delta$  symmetry one. This feature is also valid for the  $\alpha$  and  $\epsilon$  symmetry lowering modes. They were, however, considered in the self-consistent calculations and a close agreement was achieved at all temperatures for the magnetization process along the [110] axis as well as for the thermal expansion of the lattice.<sup>12</sup> The calculations in the present analysis are done exactly in the same conditions.

The strain susceptibility determines the conditions for the existence of the quadrupolar ordering: in the case of a second-order process, it occurs at a temperature  $T_Q$ , given by  $1/\chi_\delta(T_Q) = G^\delta$ . The zero-field temperature variation of  $1/\chi_\delta$  is drawn in Fig. 1. The Van Vleck behavior with a low-temperature plateau at 200 mK is associated with the singlet ground state, and the 157 mK minimum of  $1/\chi_\delta$  around 19 K results from the competition in Eq. (5) between the Van Vleck terms and the large Curie terms associated with the doublet lying at 41.6 K. Since the quadrupolar interaction coefficient  $G^\delta$  reaches only 130 mK, the lattice remains tetragonal.

It is easy to understand the  $\delta$  quadrupolar ordering stimulated by an external stress out of the  $\delta$  symmetry through the modification of the  $\delta$  strain susceptibility. From an experimental point of view, the simplest strain to apply is a magnetic field along the [100] or [001] axes. In this latter direction,  $\chi_\delta$  decreases, which made the quadrupolar ordering more difficult. On the contrary, immediately the field is applied along [100],  $1/\chi_\delta$  decreases at low temperature (Fig. 1, upper part). Note that as soon as the doublet is significantly populated,  $1/\chi_\delta$  is only weakly reduced. For fields larger than 9.4 T, the electronic system becomes overcritical and the  $\langle P_{xy} \rangle$  quadrupolar component orders at a  $T_Q$  value determined as indicated in Fig. 1 for 10 T.

The increase at low temperature of the  $\delta$  strain susceptibility by the [100] magnetic field results from the modification of both the  $P_{ik,jl}$  matrix elements and the  $(E_i - E_j)$  level spacings. Close to 0 K,  $\chi_\delta$  comes, in zero field, essentially from the matrix element between the ground state and the excited singlet at 112 K; there is no matrix element coupling with the doublet (Fig. 1, lower part). In increasing field, new components in the  $|J_z\rangle$  basis appear in the eigenfunctions: a

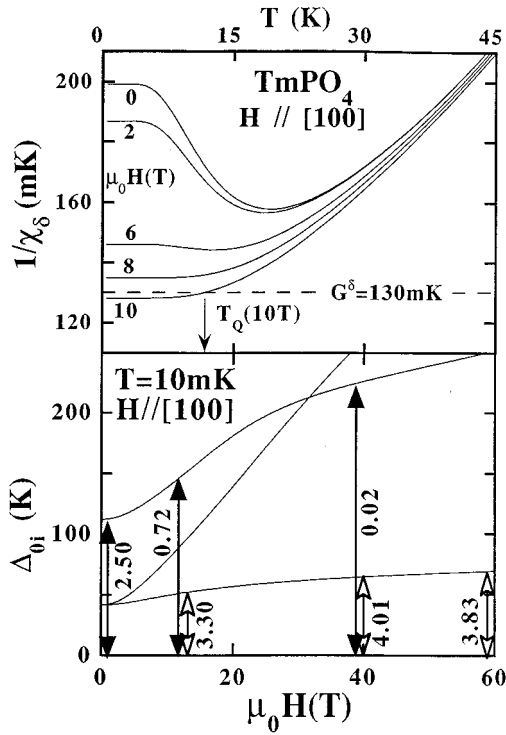


FIG. 1. Upper part: temperature variation of the reciprocal  $\chi_\delta$  strain susceptibility for magnetic fields applied along the [100] direction.  $G^\delta = 130$  mK characterizes the  $\delta$  quadrupolar interactions; the arrow gives the JT transition temperature  $T_Q$  in a field of 10 T. Lower part: field dependence of the energy of the low-lying levels with the  $|P_{ik,jl}|^2/E_i - E_j$  contributions (in  $K^{-1}$  unit) to  $\chi_\delta$  in 0, 12, 40, and 60 T at 10 mK; the energy of the singlet ground state is taken as origin.

matrix element between the ground state and one sublevel from the doublet arises. Its contribution,  $|P_{ik,jl}|^2/(E_i - E_j)$ , becomes dominant and is responsible for the decrease of  $1/\chi_\delta$  below the 130 mK critical value. In very high fields, it decreases, thus  $1/\chi_\delta$  increases above 130 mK and the electronic system turns back to the tetragonal symmetry. Note that the spacing between this sublevel and the ground state does not drastically vary, thus the JT transition is mainly stimulated through the modification of the eigenfunctions and not through a simple modification of the level spacings as usually assumed in theoretical models.

The  $\delta$  orthorhombic-tetragonal phase diagram is deduced from the equality of the  $1/\chi_\delta$  reciprocal susceptibility and the 130 mK critical value for various conditions of magnetic field and temperature (Fig. 2). The existence of two reentrant phase transitions confirms theoretical expectations obtained in Ref. 8 in terms of the ratio  $\Delta/A$  of the energy gap between quadrupolarly active electronic states,  $\Delta$ , and the intersite quadrupolar interaction,  $A$ . The phase diagram of Fig. 2 provides us with critical fields, which depend only on the  $B$ 's and  $G$ 's determined in Ref. 12. Their lowest values can be checked experimentally, as shown in the following sections.

The field dependence at 4 K of the  $\langle P_{xy} \rangle$  order parameter is drawn in Fig. 3. The two transitions are of second order. The difference between the free energies with ( $G^\delta = 130$  mK) and without ( $G^\delta = 0$  mK) quadrupolar interactions is weak, around 120 mK at its maximum. This comes from the fact that the  $-k_B T \ln Z$  change is almost compensated by the

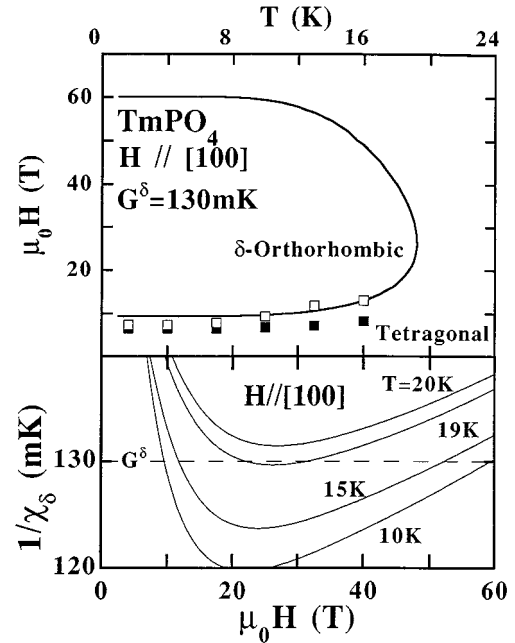


FIG. 2. Structural phase diagram for the tetragonal symmetry and the  $\delta$  orthorhombic one stimulated by a [100] magnetic field in the presence of  $\delta$  quadrupolar interactions. Open and black squares correspond to determinations by magnetostrictive and magnetic measurements, respectively. In the lower part, the existence of the quadrupolar transition is deduced from different isothermal variations of  $1/\chi_\delta(H)$ .

corrective energy,  $E_Q$ . Thus in spite of quite a sizable quadrupolar moment, the change of the free energy associated with the JT effect stimulated by the [100] field is small in comparison with the transition temperature. The weakness of this energy gain is confirmed by the angular dependence of the free energy in the basal plane (Fig. 4). The CEF anisotropy is strongly reinforced in favor of the [110] axis by the  $\delta$  quadrupolar interactions: along the [110] axis, the change of the level spacings, then of the partition function, leads to a variation of the free energy larger than the corrective energy

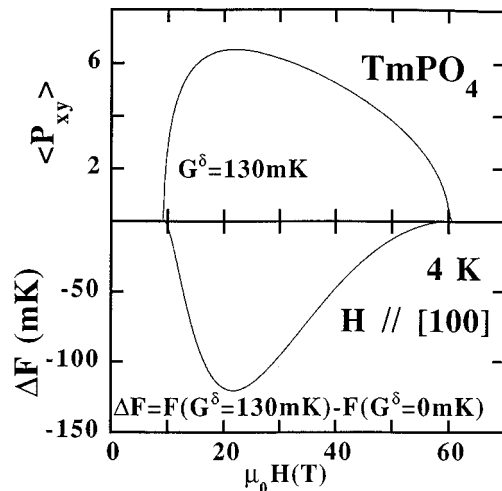


FIG. 3. Field dependence at 4 K of the  $\langle P_{xy} \rangle$  order parameter and of the difference of the free energies with and without  $\delta$  quadrupolar interactions for a [100] magnetic field.

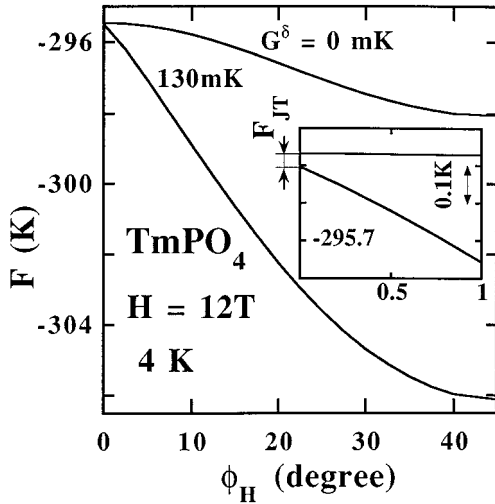


FIG. 4. The CEF free energy and the free energy in the presence of  $\delta$  quadrupolar interaction as functions of the direction of the magnetic field applied in the basal plane for a field modulus of 12 T at 4 K. The inset gives the behavior close to the [100] axis.

$E_Q$ . The existence of the stimulated JT effect is effectively a novel feature, but the inset of Fig. 4 shows how accurate the experimental conditions of the field orientation have to be in order to observe it.

### III. MAGNETIZATION IN A [100] MAGNETIC FIELD

As soon as the [100] field drives the  $\langle P_{xy} \rangle$  quadrupolar moments to order, the field direction is no longer a high-symmetry axis in a  $\delta$  orthorhombic domain and the paramagnetic moment moves away from this direction towards the [110] tetragonal one. This induces a change in the magnetic component parallel to the field and gives rise to a nonzero perpendicular component, which constitutes a direct signature of the JT cooperative effect.

Measurements of the magnetization component along the [100] field were collected in fields up to 11 T in a thermal range from 1.5 to 300 K with an accuracy better than  $0.02\mu_B$  for the magnetization and a thermal stability better than 0.01 K. Figure 5 shows in particular the field variation at 7 K, compared with the behavior observed for a [110] field (the whole set of the [110] magnetization curves is discussed in Ref. 12 through the fit of their field derivative). As explained in the Introduction, immediately the [110] field is applied, a nonzero  $\langle P_{xy} \rangle$  quadrupolar component is induced, and the inflexion point in the magnetization curve corresponds to its reinforcement by the  $\delta$  quadrupolar interactions, more or less sudden according to the temperature: this inflexion point can be considered as the boundary between the tetragonal phase and the orthorhombic  $\delta$  one, driven by the field of the corresponding symmetry. The observation of the stimulated JT effect in a [100] field is more delicate. At 19 K there is no anomaly in the experimental variation, which perfectly agrees with calculations: there is no contribution of the  $\delta$  symmetry as shown by the phase diagram of Fig. 2. At lower temperatures, i.e., below 16 K, a slight shift from the calculated behavior is observed, characterized by an anomaly on the field derivative of the magnetization around 6.5 T. This anomaly is very similar to that calculated at 9.5 T using

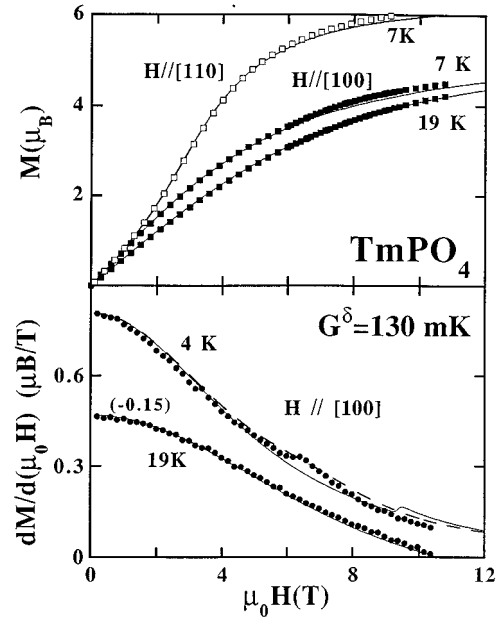


FIG. 5. Isothermal field variations of the magnetic component along the [100] field (upper part) and of its derivative (lower part); the derivative at 19 K is vertically shifted by a  $-0.15$  value. The variation obtained at 7 K along [110] is also drawn. Lines are variations calculated with  $G^\delta=130$  mK; the hatched one corresponds to a misorientation of the field,  $\phi_H=2$  degrees, away from the [100] axis in the basal plane.

$G^\delta=130$  mK. A value of 140 mK would shift the anomaly field towards the observed one. Their coincidence can be also achieved in the case of a slight misorientation of the [100] axis with respect of the applied field.

The magnetization vector was then measured in another cryomagnet as a function of the orientation of the magnetic field in the basal plane. The sample can rotate round its [001] axis perpendicular to the field. Three pairs of compensated coils measure simultaneously the flux variations parallel and perpendicular to the field during the displacement of the sample parallel to the field. The maximum field is 7.5 T, the accuracy on the magnetic components is about  $0.04\mu_B$ , the positioning angles are determined within  $\pm 0.15^\circ$  and the temperature is regulated within  $\pm 0.01$  K.

The upper part of Fig. 6 shows the two components,  $M_{\parallel H}$  and  $M_{\perp H}$ , of the paramagnetic moment during the rotation of a constant field in the basal plane. The  $\pi/2$  periodicity is perfectly respected by the two components.  $M_{\parallel H}$  is maximum (minimum) for a field along the [110] ([100]) axes. As in a torque experiment,  $M_{\perp H}$  vanishes as soon as the field points in a high-symmetry direction. The  $M_{\perp H}$  variation is sine-shaped in low fields, while being only periodic in high fields, with an extremum shifted towards the  $\langle 100 \rangle$  axes. The same analysis is valid for the  $M_{\parallel}$  variation. It exhibits an angular point along the  $\langle 100 \rangle$  axes, which becomes more and more pronounced in increasing fields. The angular variations of the two components are closely described by calculations with  $G^\delta=130$  mK. The large differences between the behaviors calculated with and without  $\delta$  quadrupolar interactions show that this technique is an efficient experimental probe for the study of quadrupolar interactions in addition to those

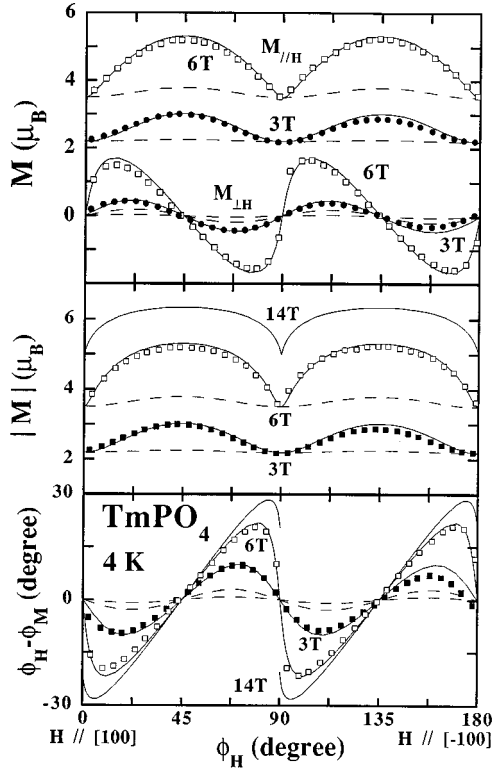


FIG. 6. Upper part: components parallel and perpendicular to the field of the paramagnetic moment as functions of the direction of the field in the basal plane. Middle part: the modulus of the paramagnetic moment as a function of the field direction. Lower part: the angle between the field and the paramagnetic moment as a function of the field direction. For 14 T, the initial values of  $M_{\perp H}$ , thus of  $\phi_H - \phi_M$  are  $1.7\mu_B$ ,  $-20.4^\circ$ , respectively. Lines are calculated with  $G^\delta = 130$  mK (solid lines) and  $G^\delta = 0$  mK (hatched lines).

of elastic constants, parastriction and third-order magnetic susceptibility.<sup>2</sup>

From the values of  $M_{\parallel H}$  and  $M_{\perp H}$ , it is possible to calculate the angle,  $\phi_H - \phi_M$ , between the field and the paramagnetic moment, as well as the modulus of this latter. The variations in the lower part of Fig. 6 show that the anisotropies of both the magnetization and the energy are strongly determined by the  $\delta$  quadrupolar interactions. Immediately  $\mathbf{H}$  is no longer parallel to the  $[100]$  axis, the moment increases, moves away from this direction and lies between the field and the  $[110]$  axis. This rotation of the paramagnetic moment exists for  $\phi_H = 0$  in fields larger than 9.5 T, i.e., in the stimulated  $\delta$  orthorhombic phase: in 14 T, the values of  $M_{\perp H}$  and  $\phi_H - \phi_M$  reach  $1.7\mu_B$  and  $-20.4^\circ$ , respectively.

The variation of  $M_{\parallel H}$  and  $M_{\perp H}$  as a function of the field are drawn for successive orientations at 4 K in Fig. 7.  $M_{\parallel H}$  is reminiscent of the behavior in Fig. 5. For  $\phi_H = 0$  degree,  $M_{\perp H}$  is zero up to the 7.5 T maximum field in agreement with the calculated curve. Note that above 9.5 T, this component would remain zero in case of an equipartition of  $\delta$  orthorhombic domains. The set of experimental variations for the indicated  $\phi_H$  values are in perfect agreement with the theory of the stimulated JT effect, although the available field is too small to allow us the direct observation of the  $\phi_H = 0$  transition.

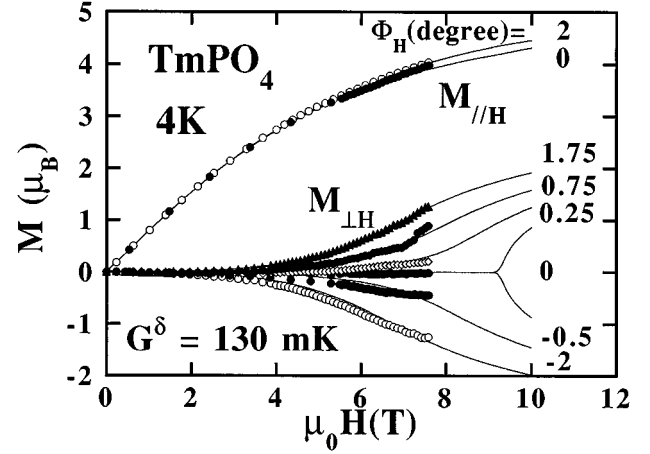


FIG. 7. Field variations of the components parallel and perpendicular to the field of the paramagnetic moment for different orientations of the applied field close to the  $[100]$  direction. Solid lines are calculated with  $G^\delta = 130$  mK. The two branches in high fields for  $\phi_H = 0$  correspond to the two possible  $\delta$  orthorhombic domains.

#### IV. MAGNETOSTRICTION ALONG THE $[100]$ DIRECTION

The relative change of length induced by a magnetic field applied in the  $(\alpha_1\alpha_2\alpha_3)$  direction and measured in the  $(\beta_1\beta_2\beta_3)$  direction is

$$\lambda_{\alpha_1\alpha_2\alpha_3}^{\beta_1\beta_2\beta_3} = \left[ \frac{\delta l}{l} \right]_{\alpha_1\alpha_2\alpha_3}^{\beta_1\beta_2\beta_3} = \frac{\epsilon^{\alpha_1}}{\sqrt{3}} + \frac{1}{\sqrt{6}} \epsilon^{\alpha_2} (2\beta_3^2 - \beta_1^2 - \beta_2^2) + \frac{1}{\sqrt{2}} \epsilon^\gamma (\beta_1^2 - \beta_2^2) + \sqrt{2} \epsilon^\delta \beta_1 \beta_2 + \sqrt{2} \beta_3 (\epsilon_1^\epsilon \beta_1 + \epsilon_2^\epsilon \beta_2). \quad (6)$$

It can be measured using strain gauges as done previously.<sup>11,12</sup> Depending on the  $(\alpha_1\alpha_2\alpha_3)$  direction, the  $\epsilon^\mu(\mathbf{H}) = B^\mu / C_0^\mu \langle O_2^\mu \rangle$  contributes or not to  $\lambda_{\alpha_1\alpha_2\alpha_3}^{\beta_1\beta_2\beta_3} \cdot \epsilon^\delta(\epsilon^\gamma)$  is zero for a magnetic field strictly applied along the  $[100]$  ( $[110]$ ) axis. In the case of even a slight misorientation of the field away from the  $[100]$  axis, a sizable  $\langle P_{xy} \rangle$  value is immediately induced and, owing to the large  $B^\delta / C_0^\delta$  ratio, the resulting  $\epsilon^\delta$  contribution overwhelms the other ones in  $\text{TmPO}_4$ . As in the magnetization processes discussed previously, the stimulated JT effect is hidden by the metamagneticlike behavior:  $\epsilon^\delta$ , thus  $\lambda_{100}^{\beta_1\beta_2\beta_3}$  exhibits an S-shaped field dependence in small magnetic fields instead of the  $\langle P_{xy} \rangle$  behavior drawn in Fig. 3. Then when searching for the intrinsic stimulated JT effect, the best way is to eliminate the  $\delta$  contribution in Eq. (6) by gluing the strain gauge along the  $[100]$  axis in the  $(010)$  plane, using the fact that it is a cleavage plane. The relative change of length reduces to  $\epsilon_a = \lambda_{100}^{\beta_1\beta_2\beta_3} = \epsilon^{\alpha_1} / \sqrt{3} - 1 / \sqrt{6} \epsilon^{\alpha_2} + 1 / \sqrt{2} \epsilon^\gamma$ . An anomaly in its field dependence is then the signature of the reconstruction at the JT transition of the level spectrum and the eigenfunctions, the experimental difficulties being in the field alignment parallel to the  $[100]$  axis and in the measurement of small changes of length. Data in fields up to 14 T are given in Fig. 8. The magnetostrictive signals are small, less than 90 ppm.

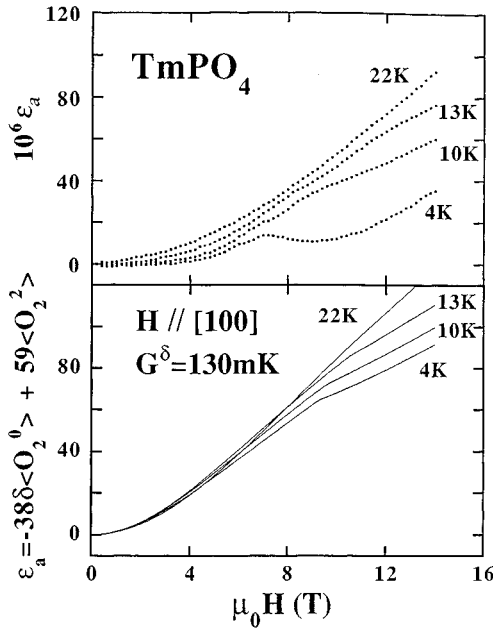


FIG. 8. Relative changes of length induced along the [100] direction by a [100] magnetic field at various temperatures (upper part: data, lower part: variations calculated with the magnetoelastic coefficients determined at high temperature).

Anomalies are observed in the  $\epsilon_a$  field dependence for temperatures lower than 19 K, the corresponding field values are reported on the phase diagram in Fig. 2. In agreement with this, a simple quadratic behavior is observed at higher temperatures. The  $\epsilon_a$  field variation can be described as soon as the different strain contributions are known:  $\epsilon^\gamma(H) = B^\gamma/C_0^\gamma \langle P_{xy}(H) \rangle$  and  $\epsilon^{ai}(H) = A^{ai} [\langle O_2^i(H) \rangle - \langle O_2^i(0) \rangle]$  with  $A^{a1}$  and  $A^{a2}$  being the combinations of the  $B^{a1}$  and  $B^{a2}$  magnetoelastic coefficients and the  $C_0^{a1}$ ,  $C_0^{a2}$ , and  $C_0^{a12}$  elastic constants.<sup>15</sup>  $A^{a2} = 47$  and  $(1/\sqrt{2})(B^\gamma/C_0^\gamma) = 59$  ppm were determined in Ref. 12. Different measurements, not presented here, confirm these values and give  $A^{a1} = -32$  ppm. The variations calculated with  $G^\delta = 130$  mK are compared in Fig. 8 with the data, the general behavior of which is well described. However the magnitude of the  $\epsilon_a$  strain is calculated globally 30% larger than measured, the anomaly at the critical field is less pronounced than the observed one. These differences in addition with the slightly negative  $\epsilon_a$  variation in low fields below 10 K indicate additional contributions. For instance, a parasitic  $\delta$  contribution  $[\sqrt{2}(B^\delta/C_0^\delta) = -1100$  ppm] can explain the 30% reduction of the experimental value if misorientations of  $2^\circ$  and  $0.15^\circ$  out of the [100] axis are assumed for the magnetic field and the gauge, respectively. However stresses introduced by the necessary gluing of the sample as well as anharmonic couplings between magnetoelastic modes could also contribute to this reduction of the data.

## V. CONCLUSION

The theoretical model of the stimulated cooperative JT effect presented in Refs. 7 and 8 has been quantitatively developed considering all the features of the CEF in the ground-state multiplet and all the various magnetoelastic couplings. It was applied to the case of  $\text{TmPO}_4$ , for which all

the coefficients are known, thus without any adjustable parameter. The structural phase diagram for the tetragonal phase and the  $\delta$  orthorhombic one is deduced from the analysis of the  $\delta$  strain susceptibility as a function of the temperature and the magnetic field, as normally done in the MFA. The mechanism of the stimulated JT effect is not a simple modification of the energy spacing between the singlet ground state and the excited levels quadrupolarly active, but essentially a field reconstruction of the eigenfunctions, which introduces additional matrix elements and then reinforces the  $\delta$  strain susceptibility: the JT effect occurs as soon as the critical value,  $G^\delta = 1/\chi_\delta(T_Q)$  is reached. The reentrant feature of the structural phase diagram, i.e., the occurrence at high field of a second transition, from the orthorhombic  $\delta$  symmetry back to the tetragonal one, is driven by the decrease of the matrix elements rather than by a change of the energy spacings.

This JT effect stimulated by a magnetic field applied out of the quadrupolar symmetry is a phenomenon from a theoretical point of view. However the free-energy gain associated with the quadrupolar ordering is weak in comparison with the gain in a field, when this field belongs to the same symmetry. The same conclusion is valid for the magnitude of the quadrupolar component: to apply in  $\text{TmPO}_4$  a field of a given strength along the [100] axis is much less efficient than along the [110] one.

From an experimental point of view, the main consequence is that the conditions of parallelism between the external field and the [100] direction are severe in order to observe the intrinsic stimulated JT effect. At the structural temperature  $T_Q$ , the change of the component parallel to the field of the paramagnetic moment is weak and manifests itself only through a small increase of the field derivative. Measured and calculated values of the critical field are in agreement. They become equal, assuming a misorientation of  $2^\circ$  or leaving the  $G^\delta$  coefficient free to vary in its uncertainty range.

The main modification of the paramagnetic moment at the stimulated transition is its large rotation away from the [100] field direction towards the [110] one associated with the  $\langle P_{xy} \rangle$  quadrupolar ordering. The study of the magnetic vector at different temperatures according to the positioning angle as well as to the field strength agrees perfectly with the calculations, although the available field does not allow us to observe the intrinsic stimulated JT effect in  $\text{TmPO}_4$ . This experimental technique, which simultaneously measures the parallel and perpendicular components of the magnetic vector as functions of the positioning angle is a fruitful experimental probe with respect to quadrupolar interactions. In  $\text{TmPO}_4$ , it confirms the  $G^\delta = 130$  mK value in close agreement with the preceding determinations.<sup>12</sup>

In the present magnetostriction measurements, the positioning angle of the field is not monitored with the same accuracy as in the magnetic measurements. In the case of a misorientation, even slight, the  $\delta$  strain is induced immediately the field is applied and the intrinsic stimulated JT effect is hidden. To minimize, if not eliminate, the  $\delta$  contribution, the appropriate geometry is to glue the gauge along the [100] axis in the natural (010) plane and to observe the cooperative JT effect through the changes in the  $\alpha$  and  $\gamma$  strains. The values of the critical field are close to those observed in the magnetic measurements. Both sets of experimental values

correctly describe the low-field limit between the tetragonal and orthorhombic phases experimentally obtainable in the calculated structural phase diagram.

This observation of the stimulated JT effect in  $\text{TmPO}_4$  shows that the experimental procedure is very delicate, at least in this system. This is due to the fact that the intrinsic effect is easily hidden by the usual metamagneticlike behavior when there is a misorientation. A remaining question is to know if the weak gain in free energy in the stimulated orthorhombic phase is only characteristic of  $\text{TmPO}_4$  or if it is a general feature. A possible answer may be expected from similar studies in the  $\text{Tb}_x\text{Gd}_{1-x}\text{VO}_4$  system, where the dilu-

tion may allow one to monitor the undercritical state more or less close to criticality and in this way to reduce the critical field values.

#### ACKNOWLEDGMENTS

The Laboratoire Louis-Néel is associated with the Université Joseph-Fourier, Grenoble. This research is supported, in part, by the Russian Fundamental Science Foundation. Z.K. wants to thank the Ministère de l'Enseignement Supérieur et de la Recherche for its support and the Laboratoire Louis-Néel for its hospitality.

- 
- <sup>1</sup>G. A. Gehring and K. A. Gehring, *Rep. Prog. Phys.* **38**, 1 (1975).  
<sup>2</sup>P. Morin and D. Schmitt, in *Ferromagnetic Materials*, edited by K. H. J. Buschow and E. P. Wohlfarth (North-Holland, Amsterdam, 1990), Vol. 5, p. 1.  
<sup>3</sup>P. Morin and J. Rouchy, *Phys. Rev. B* **48**, 256 (1993).  
<sup>4</sup>D. P. Clougherty, K. H. Johnston, and M. E. McHenry, *Physica C* **162-164**, 1475 (1989).  
<sup>5</sup>M. Schluter, M. Lannoo, M. Needels, G. A. Baraff, and D. Tománek, *Phys. Rev. Lett.* **68**, 526 (1992).  
<sup>6</sup>A. J. Millis, B. I. Shraiman, and R. Mueller, *Phys. Rev. Lett.* **77**, 175 (1996).  
<sup>7</sup>B. G. Vekhter, V. N. Golubev, and M. D. Kaplan, *JETP Lett.* **45**, 168 (1987).  
<sup>8</sup>M. D. Kaplan and G. O. Zimmerman, *Phys. Rev. B* **52**, 1 (1995).  
<sup>9</sup>K. D. Knoll, *Phys. Status Solidi B* **45**, 553 (1971); C.-K. Loong, L. Soderholm, G. L. Goodman, M. M. Abraham, and L. A. Boatner, *Phys. Rev. B* **48**, 6124 (1993).  
<sup>10</sup>R. T. Harley and D. I. J. Manning, *J. Phys. C* **11**, L633 (1978).  
<sup>11</sup>P. Morin, J. Rouchy, and Z. Kazei, *Phys. Rev. B* **50**, 12 625 (1994).  
<sup>12</sup>P. Morin, J. Rouchy, and Z. Kazei, *J. Phys. C* **87**, 967 (1996).  
<sup>13</sup>K. W. H. Stevens, *Proc. Phys. Soc. London Ser. A* **65**, 209 (1952).  
<sup>14</sup>E. du Trémolet de Lacheisserie, *Ann. Phys.* **5**, 267 (1970).  
<sup>15</sup>P. Morin, J. Rouchy, and D. Schmitt, *Phys. Rev. B* **37**, 5401 (1988).